D-type cyclins activate division in the root apex to promote seed germination in *Arabidopsis*

Nompumelelo H. Masubelele*†, Walter Dewitte*, Margit Menges*, Spencer Maughan, Carl Collins, Rachael Huntley‡, Jeroen Nieuwland, Simon Scofield, and James A. H. Murray§

Institute of Biotechnology, University of Cambridge, Tennis Court Road, CB2 1QT Cambridge, United Kingdom

Communicated by Brian A. Larkins, University of Arizona, Tucson, AZ, September 7, 2005 (received for review July 16, 2005)

Seeds provide survival and dispersal capabilities by protecting the dormant mature plant embryo. Germination and resumption of development under favourable conditions requires the reinitiation of cell growth and division through poorly understood processes. Here we show that four phases of cell division activation during germination in *Arabidopsis* are related to external morphological changes. Cell division initiates in the root apical meristem (RAM) before root protrusion, followed by sequential activation of cell division in the cotyledons, shoot apical meristem (SAM), and secondary meristems. Major changes in transcript levels of >2,000 genes precede root emergence, including expression peaks of six D-type (CYCD) and two A-type cyclins. Two further CYCDs are activated later with the SAM. Early activated CYCDs play key roles in regulating the extent of cell division, because loss-of-function alleles of early CYCDs display reduced division activation and consequential delayed root emergence. Conversely, elevation of early CYCDs increases cell cycle activation in the RAM and promotes embryonic root (radicle) protrusion, whereas a later-acting CYCD does not. These phenotypes, together with their overlapping expression domains, support a cumulative action of a subset of CYCDs in cell cycle reactivation, rather than a complete functional redundancy. This analysis reveals a phenotype associated with loss-of-function of a plant cyclin and demonstrates that D-type cyclins regulate cell cycle reentry during meristem activation to promote successful germination and early seedling growth.

cell cycle | cyclin D

The dormant plant embryo in the form of seeds allows survival of the plant under suboptimal conditions and facilitates dispersal. The ensuing process of seed germination is thus both vital to plant development and of key agronomic importance. Germination entails the resumption of growth and development by a complex series of processes triggered by water uptake by the quiescent dry seed and is generally considered to be complete when the radicle penetrates the seed coat (1, 2). The first signs of germination are the resumption of essential metabolic processes, including transcription, translation, and DNA repair; this is followed by directional cell expansion, and eventually the activation of cell division in the root (RAM) and shoot (SAM) apical meristems (3, 4). In postgermination growth, the production of additional cells in the apical meristems and their expansion drives root and stem growth, as well as the subsequent formation of lateral organs. However the role of cell division activation in the germination process itself remains unclear, as the radicle has been shown to be able to grow to a certain extent and protrude from the seed coat in the absence of cell cycle activity (5, 6), and cell division is generally considered to occur only at the completion of germination as classically defined by radicle emergence (1). However, in germinating seeds of certain species such as tobacco, tomato, and conifers, cell division activation has been found to precede radicle protrusion (1, 7, 8).

Eukaryotic cell division is driven by the consecutive action of cyclin/cyclin-dependent kinase (CYC/CDK) complexes, whose activity is further regulated by phosphorylation and interaction with inhibitor and scaffolding proteins (9). Plants contain both conserved and plant-specific regulators, including a unique class of CDKB showing cell cycle regulated expression in G_2/M (10). Cyclin classes are conserved with mammals; although cyclin E is absent, other types have abundant members, and *Arabidopsis* encodes 10 A-type cyclins in three subgroups (CYCA1–3), 11 B-type cyclins in three subgroups (CYCB1–3), and 10 CYCD in seven subgroups (CYCD1–7) (11, 12). CDK inhibitor proteins are represented by seven proteins with limited homology to the mammalian inhibitor $p27^{KIP1}$, known as Kip-related proteins.

Regardless of the definition of germination, activation of cell division in the root and shoot meristem is vital for seedling development. Examining *Arabidopsis thaliana* during germination and seedling growth revealed four distinct phases defined by morphological changes, cell division activation, and gene expression profiles. Cell cycle activation in the root meristem precedes seed coat protrusion and is accompanied by major changes in transcript levels. We identify a subset of early-activated D- and A-type cyclins as putative mediators of cell cycle reentry and show, using both mutant and overexpression analysis, that early activated D-type cyclins are rate limiting for cell cycle activation in the root meristem and subsequent radicle protrusion. These observations suggest a contributing role of cell division to radicle growth during germination in *Arabidopsis* and provide genetic evidence that D-type cyclins promote cell cycle reentry in developmental contexts.

Materials and Methods

Plant Material. The wild-type (WT) *Arabidopsis thaliana* ecotypes Columbia (Col-0), diploid and tetraploid lines of Landsberg *erecta* (L*er*), Cape Verde Islands (Cvi-0), and Wassilewskija (Ws-0) were obtained from the Nottingham *Arabidopsis* Stock Centre, and all comparisons were made on coharvested seed. Constitutive (35S CaMV promoter) *CYCD2;1* and *CYCD3;1* overexpressing (OE) lines were constructed as described (refs. 13 and 14; see also *Supporting Text*, *Data Set*, and Figs. 4–6, which are published as supporting information on the PNAS web site). Loss-of-function *cycd1;1* and *cycd4;1* mutants were recovered from the GABI-Kat (15) and Salk collections (16), respectively. The *cycd4;1–1* mutant line (TAIR accession no. 015525) has a T-DNA insertion at position −25 bp from the initiation codon, and *cycd1;1* (TAIR accession no. AL766879) has a T-DNA insertion in the second intron. In both cases, the absence of the *CYCD* transcript was confirmed by RT-PCR. *cycd4;1* was backcrossed twice to Columbia WT, and WT segregants were used as controls in all experiments. Homozygote *cycd1;1* Co-

Abbreviations: RAM, root apical meristem; SAM, shoot apical meristem; CYC, cyclin; CDK, cyclin-dependent kinase; GUS, β-glucuronidase; SLR, signal log ratio; OE, overexpressors.

*N.H.M., W.D., and M.M. contributed equally to this work.

†Present address: Biotechnology Division, ARC-Roodeplaat Vegetable and Ornamental Plant Institute, Private Bag X293, Pretoria 0001, South Africa.

‡Present address: Department of Plant Biology, Carnegie Institution of Washington and Department of Biological Sciences, Stanford University, 260 Panama Street, Stanford, CA 94305.

§To whom correspondence should be addressed. E-mail: j.murray@biotech.cam.ac.uk.

lumbia lines were compared to WT seed batches harvested at the same time.

pCYCD1;1::β-glucuronidase (GUS) and pCYCD4;1::GUS reporter lines containing 3,082 and 2,414 bp of the promoter sequences of *CYCD1;1* and *CYCD4;1* driving GUS, respectively, were constructed by using Gateway cloning of the PCR-amplified promoter fragments (Invitrogen) in the pKGWFS7 target vector (Plant Systems Biology, Ghent, Belgium). pCYCD3;1 includes the full upstream sequence of *CYCD3;1* (≈1 kb) as described (supporting information).

Growth Conditions and Seed Germination Assays. *Arabidopsis thaliana* L*er* expressing the pCYCB1;1::DB-GUS fusion protein under control of the *CYCB1;1* promoter (gift of P. Doerner, University of Edinburgh, Edinburgh, U.K.), was used for both the analysis of cell cycle activation and subsequent transcript profiling analysis using GeneChips arrays. For all experiments, seeds were sown on a double layer of prewetted filter paper, and stratified at 4°C for 3 days in the dark to ensure synchronous germination before moving to Conviron TC30 cabinets (Controlled Environments, Manitoba, Canada) under continuous white light (170–200 μmol m^{-2}·s^{-1}) at 22°C on moist filter paper.

For germination assays, seeds together with controls were arranged in square Petri plates with >100 seeds each, and grown vertically. Images were recorded over time and scored for radicle protrusion up to 28 h after germination. For germination assays using cell cycle specific inhibitors, aphidicolin was added to a final concentration of 12 μg/ml or roscovitine to a final concentration of 100 μM, and germinating seeds were scored up to 44 h.

GUS Staining. To identify mitotic cells, a fusion of the promoter and destruction box of the mitotic cyclin *CYCB1;1* to GUS (pCYCB1;1::DB-GUS) that is expressed only in cells during G_2/M and destroyed in mitosis (17) was used. Histochemical GUS staining was performed on whole embryos and seedlings essentially as described (18) for germinating seeds carrying the pCYCB1;1::DB-GUS, pCYCD1;1::GUS, pCYCD4;1::GUS, pCYCD3;1::GUS or 35S::CYCD3;1 and pCYCB1;1-DB::GUS constructs under the growth conditions described above. The stained embryos were cleared in Hoyer's solution (19) and examined with a Nikon Optiphot microscope equipped with a digital camera.

Flow Cytometry to Determine DNA Distribution. Samples of >100 mature embryos were isolated from the seed coats and harvested at the different stages of germination. Nuclei were released by chopping and analyzed as described (20).

Cell Cycle Activation Assay in Root Meristems. Germinating embryos and seedlings were fixed overnight in FAA (3.7% paraformaldehyde/81% EtOH/5% glacial acetic acid), rinsed with water, and mounted under cover slips. After crushing, the samples were snap-frozen with liquid nitrogen to allow the removal of the coverslip and mounted in Vectashield with DAPI (Vector Laboratories, Burlingame, CA). The samples were examined with a Zeiss LSM 510 Meta confocal microscope, and the number of metaphases and anaphases were scored for each root. At least 10 roots were counted for each sample.

RNA Preparation and High-Density Oligonucleotides Array Hybridization. Total RNA was prepared from WT mature embryos of different morphological stages during seed germination by using Tri-Pure isolation reagent (Boehringer-Mannheim) according to manufacturer's instructions. Embryos were dissected from their seed coat and harvested at nine time points, including end of imbibition (T0) and at 12, 21, 30, 33, 36, 42, 48, and 63 h after germination. Two fully independent biological replicates were prepared for each time point and grouped into time course A (series A) and time course B (series B). RNA samples were used for preparation of cDNA and biotin-labeled cRNA, and hybridization to the *Arabidopsis* full genome ATH1 GeneChip array (performed by VBC Genomics Bioscience Research, Vienna).

Bioinformatic Analysis. Raw data were processed with MASUITE 5.0 analysis software (Affymetrix). Genes were selected for further analysis if they (*i*) were called present at least once in both independent experiments (series A and series B); (*ii*) were at least once changed among the samples ("difference" call); (*iii*) were robustly regulated [only genes that showed in each duplicate of pairwise comparisons to the T0 sample the same "difference" call (series A compared to A; series B compared to B) were considered as robustly regulated]; and (*iv*) showed a 3-fold change (FC) in expression (based on averaged signal log ratios (SLR) series A and B). This analysis resulted in a data set of 3,231 genes showing robustly significant regulated expression (≥3FC) during seed germination.

The average SLR (based on series A and B) was used to analyze the variance of expression level of each gene across the time course by using standard statistical approaches (21). To calculate relative expression profiles, processed values for averaged SLR (*Xi*) were centered across the arrays, and for each gene the variance normalized SLR (*X*norm) at time *i* was determined as follow: *X*norm = (*Xi* - *X*average)/SD. Variance normalized SLR values were subjected to hierarchical cluster analysis by using GENEMATHS (version 2.01; ref. 22).

Core cell cycle genes were defined as expressed if they showed ≥1 P call in series A and ≥1 P call in series B. The average of absolute detected signals (based on series A and B) of expressed core cell cycle genes were normalized by dividing the signal by the mean, and then used for hierarchical cluster analysis using GENEMATHS (version 2.01). A coefficient of variation (CV) was calculated by dividing the standard deviation by the mean signal (CV = SD/average).

Results and Discussion

Activation of Cell Division in Germination and Seedling Growth. We examined germination and associated activation of cell division in *Arabidopsis thaliana* L*er* using morphological characterization, flow cytometry, and a mitotic cyclin (*CYCB1;1*) fusion to GUS to report mitotic cells (17). This construct (pCYCB1;1::DB-GUS) fuses the promoter and first exon of *CYCB1;1* to GUS, and the resulting inclusion of the CYCB destruction box on the GUS protein creates an unstable GUS protein present only in cells in G_2 and early M phase of the cell cycle. We found that consecutive events during the initial phases of postembryonic plant growth can be divided into four sequential phases. In phase I, no mitotic cells or externally visible morphological changes are observed (Fig. 1*A*). In this phase, cells resume metabolic activity (3, 23) and reassemble the microtubular cytoskeleton (7, 8), and cell expansion alone drives the growth of the embryo. Cells of the embryo have a 2C DNA content, confirming that they are largely in the G_1 phase of the cell cycle (Fig. 1*B*).

Phase II is defined by activation of cell division in the root apex, which we found always shortly precedes the protrusion of the embryonic root or radicle through the seed coat (Fig. 1*A*). These first cell divisions in *A. thaliana* L*er* expressing the mitotic marker pCYCB1;1::DB-GUS occur 21 h after stratification in the outer cell layers of the root tip within the lateral root cap (Fig. 1*C a* and *b*) or the epidermis. Activation of cell proliferation gradually extends toward the center of the root (Fig. 1*C c–h*). During this phase, nuclei with 2C, 4C, and 8C DNA contents were detected (Fig. 1*B*, T30) indicating that some cells immediately endoreduplicate their DNA, whereas cells of the RAM undergo mitotic cycles.

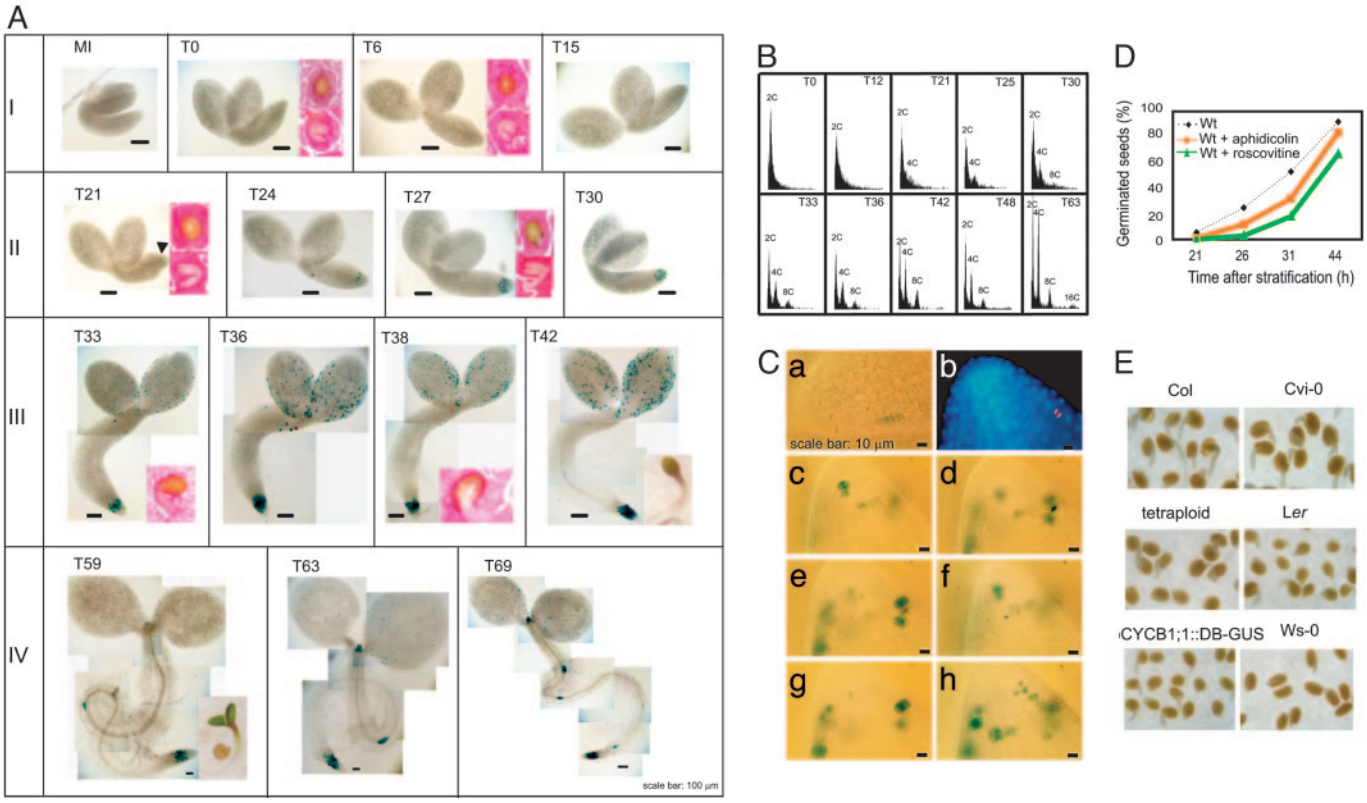

Fig. 1. Seed germination involves four distinct phases of cell cycle activation. (*A*) Sequential phases (I–IV) of cell cycle activation and related morphological events of germination. Mitotic activity is revealed by expression of the pCYCB1::DB-GUS reporter, resulting in a blue reaction product. Samples were taken from mid-imbibition (MI), at the end of stratification (T0), and at different times after placing at 22°C (*T* in hours). *Insets* (pink background) show the corresponding seed phenotype (*Upper*) and dissected embryo (*Lower*) at each time point. Phase I, expansion of embryo but no mitotic cells or external morphological change; phase II, activation of cell division in the RAM (indicated by arrowhead in T21 panel), accompanied by tearing of the seed coat and root protrusion (radicle emergence); phase III, activation of cell division in the cotyledons and SAM, continued division in the RAM and growth of the primary root, accompanied by emergence of the cotyledons; phase IV, cessation of cell proliferation in the cotyledons, initiation of division in leaf primordia in SAM and activation of lateral root primordia, accompanied by opening and greening of the cotyledons. (*B*) Changes in nuclear ploidy levels during germination. Histograms representing flow cytometry analysis of time points indicated in hours after placing seeds at 22°C. 2C peak, G_1 DNA content; 4C peak, G_2 DNA content; 8C and 16C peaks, endoreduplicating cells. Note appearance of an 8C peak at 30 h. (*C*) Detailed localization of mitotic activation in the RAM. GUS (*a*) and DAPI-staining (*b*) of the first mitotic events in the root tip at 21 h. Sequential optical sections through the RAM reveals mitotic divisions in the outer and underlying cells at 24 h (*c*-*h*) using the pCYCB1::DB-GUS reporter. (*D*) Inhibitory effect of aphidicolin and roscovitine on radicle protrusion during seed germination. (*E*) Different *Arabidopsis* ecotypes and tetraploids have different germination rates. Germinating seeds were pictured at 30 h illustrating the different extents of radicle emergence and growth.

In phase III, 12 h after activation of cell division in the root apex, cell proliferation is transiently activated in the cotyledons, and the first cells start to divide in the shoot apical meristem. At the end of phase III, the cotyledons emerge from the seed coat and commence greening. Phase IV is defined by cessation of mitotic division and final expansion of cotyledons and the initiation of lateral organs, as leaf primordia form in the SAM accompanied by a further increase in cell division activity, and the first lateral roots initiate from the root pericycle (Fig. 1*A*, T59).

Examination of a range of ecotypes showed that this description appears universal in *Arabidopsis*, with the same sequence of events and mitotic patterning being observed in the Columbia ecotype (data not shown), although with a compressed time scale because overall germination was faster in this background. Columbia (Col) proved to be the fastest germinating ecotype in comparison to other ecotypes tested (Cvi, L*er*, WS) and a L*er* tetraploid (Fig. 1*E*).

These observations indicate that exit from G_1 phase, entry into S phase, and cell division in a subset of cells in the root meristem precedes radicle protrusion in *Arabidopsis*, in contrast to the generally held view (1).

Both the mitotic cell cycle and endocycles depend on the activity of CDKs, which is efficiently inhibited in plants by the compound roscovitine that blocks cell cycle progression in both G_1 and G_2 phases (24). Progression through S phase can also be prevented by the DNA polymerase inhibitor aphidicolin (13, 25). To establish whether cell division activation and progression through the cell cycle has a role in the germination process, we examined the effects of aphidicolin and roscovitine. Both compounds significantly delayed radicle emergence and germination (Fig. 1*D*), with roscovitine showing a stronger effect, indicating that both CDK activity and DNA synthesis contribute to the elongation of the radicle during its emergence. Using the pCYCB1;1::DB-GUS line, we found that roscovitine treatment was unable to block division completely, and we observed mitotic cells in the root at 26 h, shortly before the first radicle protrusion events (data not shown). Hence, the delay in germination caused by roscovitine treatment correlated with the extent of the delay in the appearance of mitotic cells, suggesting that initiation of cell division is important in radicle emergence.

Germination and Seedling Growth Involves Major Changes in Transcript Levels. The externally visible morphological landmarks of seed germination are thus linked to a conserved pattern of cell

cycle activity as different meristems are activated, and this activation plays a role in the emergence of the root during germination. However, our understanding of the molecular pathways linking cell cycle controls with germination remains enigmatic (26). To gain insight into this mechanism, we examined transcript levels of 24,000 genes by using Affymetrix ATH1 GeneChip arrays at nine time points spanning phases I to IV in duplicate independent time courses of germinating embryos dissected from their surrounding seed coat (Fig. 4). Using stringent filtering criteria including a change in expression of at least three-fold in both duplicate experiments (*Materials and Methods*), 3,231 genes were found to be regulated during phases I–IV (*Data Set*), and hierarchical tree clustering identified seven nodes corresponding to a characteristic pattern of sequential gene activation in each phase of activation (Fig. 5). Particularly notable is that 2,600 genes show major regulation of transcript abundance before radicle emergence, which occurs at the end of phase II, and around half of these genes are highly regulated before the onset of any cell division at ≈21 h.

Core Cell Cycle Regulators Are Differentially Regulated During Germination. To identify cell cycle genes involved in meristem activation and germination, we examined transcript profiles of core cell cycle regulators. Of 87 core cell cycle regulators previously defined (27), 81 are represented by array probes, and expression of 74 of these (91%) is detected during germination (Fig. 2). Different cell cycle regulators show distinct expression patterns in germination (Fig. 2), and during phase I, before the activation of cell division within the RAM, transcription of six D-type (CYCD) and two A-type (CYCA) cyclins is up-regulated (*CYCA3;4* and *CYCA1;2*). Of the CYCD genes up-regulated during phase I, *CYCD3;2*, *CYCD3;3* and *CYCD4;1* peak within phase I, and *CYCD1;1* and *CYCD2;1* peak at the first time point within phase II, and we define these six genes as "early-activated" CYCDs. This is accompanied by regulation of other potential G_1/S phase regulators including Kip-related proteins and genes encoding subunits of CDK activating kinases (CDKD, CDKF, and CYCH).

Other D-type (*CYCD3;1*, *CYCD6;1*, and *CYCD4;2*) and A-type cyclins (*CYCA1;1*, *CYCA2;1*, and *CYCA2;3*) reach maximum levels during or at the end of phase III and are therefore defined as "late-activated." The highest overall mitotic activity was detected during phase III, and transcript levels of genes implicated in the G_2/M transition and mitosis, such as CYCBs and CDKBs, reach maximum values at this point.

These data suggest that sequential waves of cyclin/CDK expression involving specific CYCDs and CYCAs are associated with cell cycle activation in meristems during germination, presumably reflecting the sequential activation of root, shoot, and lateral meristems.

CYCDs Are Rate Limiting for Cell Cycle Activation in the Root Meristem and Seed Germination. To ascertain further the role of different CYCD relating to activation of the RAM and SAM, we examined the expression patterns of the "early" genes *CYCD4;1* and *CYCD1;1* by using GUS reporters. This finding confirmed the pattern, timing, and consecutive activation of *CYCD4;1* and *CYCD1;1* transcription during phase I and at the start of phase II in the root tip (Fig. 3*A*), and showed clearly the transient nature of *CYCD4;1* expression at T12 and *CYCD1;1* at both T12 and T21, mirroring and confirming the microarray results (Fig. 2). In contrast, expression of late-activated *CYCD3;1* was absent from the RAM during phase II (data not shown) but highly expressed in the active SAM and incipient primordia (28), again consistent with its activation in phase III (Fig. 3*B*).

CYCDs play important roles in controlling the cell cycle responses of cells in culture to stimuli such as sucrose and hormones (14, 29). To determine the roles of CYCDs in germination, we isolated homozygous loss-of-function mutants

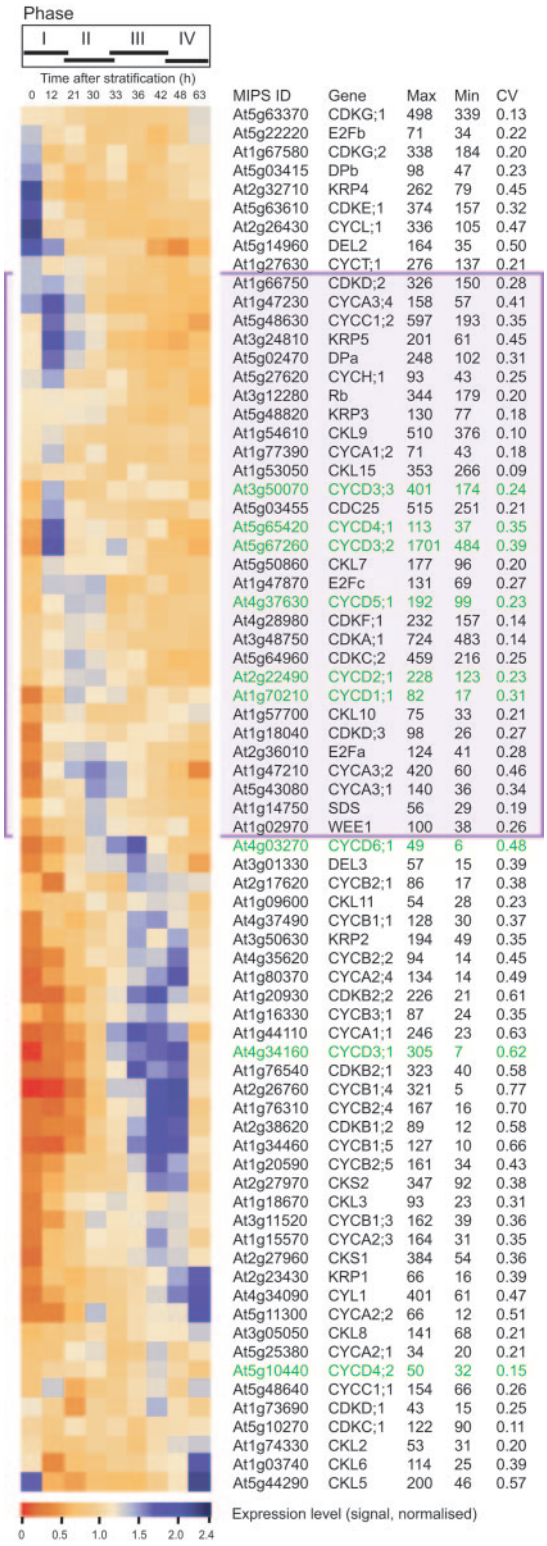

MIPS ID	Gene	Max	Min	CV
At5g63370	CDKG;1	498	339	0.13
At5g22220	E2Fb	71	34	0.22
At1g67580	CDKG;2	338	184	0.20
At5g03415	DPb	98	47	0.23
At2g32710	KRP4	262	79	0.45
At5g63610	CDKE;1	374	157	0.32
At2g26430	CYCL;1	336	105	0.47
At5g14960	DEL2	164	35	0.50
At1g27630	CYCT;1	276	137	0.21
At1g66750	CDKD;2	326	150	0.28
At1g47230	CYCA3;4	158	57	0.41
At5g48630	CYCC1;2	597	193	0.35
At3g24810	KRP5	201	61	0.45
At5g02470	DPa	248	102	0.31
At5g27620	CYCH;1	93	43	0.25
At3g12280	Rb	344	179	0.20
At5g48820	KRP3	130	77	0.18
At1g54610	CKL9	510	376	0.10
At1g77390	CYCA1;2	71	43	0.18
At1g53050	CKL15	353	266	0.09
At3g50070	CYCD3;3	401	174	0.24
At5g03455	CDC25	515	251	0.21
At5g65420	CYCD4;1	113	37	0.35
At5g67260	CYCD3;2	1701	484	0.39
At5g50860	CKL7	177	96	0.20
At1g47870	E2Fc	131	69	0.27
At4g37630	CYCD5;1	192	99	0.23
At4g28980	CDKF;1	232	157	0.14
At3g48750	CDKA;1	724	483	0.14
At5g64960	CDKC;2	459	216	0.25
At2g22490	CYCD2;1	228	123	0.23
At1g70210	CYCD1;1	82	17	0.31
At1g57700	CKL10	75	33	0.21
At1g18040	CDKD;3	98	26	0.27
At2g36010	E2Fa	124	41	0.28
At1g47210	CYCA3;2	420	60	0.46
At5g43080	CYCA3;1	140	36	0.34
At1g14750	SDS	56	29	0.19
At1g02970	WEE1	100	38	0.26
At4g03270	CYCD6;1	49	6	0.48
At3g01330	DEL3	57	15	0.39
At2g17620	CYCB2;1	86	17	0.38
At1g09600	CKL11	54	28	0.23
At4g37490	CYCB1;1	128	30	0.37
At3g50630	KRP2	194	49	0.35
At4g35620	CYCB2;2	94	14	0.45
At1g80370	CYCA2;4	134	14	0.49
At1g20930	CDKB2;2	226	21	0.61
At1g16330	CYCB3;1	87	24	0.35
At1g44110	CYCA1;1	246	23	0.63
At4g34160	CYCD3;1	305	7	0.62
At1g76540	CDKB2;1	323	40	0.58
At2g26760	CYCB1;4	321	5	0.77
At1g76310	CYCB2;4	167	16	0.70
At2g38620	CDKB1;2	89	12	0.58
At1g34460	CYCB1;5	127	10	0.66
At1g20590	CYCB2;5	161	34	0.43
At2g27970	CKS2	347	92	0.38
At1g18670	CKL3	93	23	0.31
At3g11520	CYCB1;3	162	39	0.36
At1g15570	CYCA2;3	164	31	0.35
At2g27960	CKS1	384	54	0.36
At2g23430	KRP1	66	16	0.39
At4g34090	CYL1	401	61	0.47
At5g11300	CYCA2;2	66	12	0.51
At3g05050	CKL8	141	68	0.21
At5g25380	CYCA2;1	34	20	0.21
At5g10440	CYCD4;2	50	32	0.15
At5g48640	CYCC1;1	154	66	0.26
At1g73690	CDKD;1	43	15	0.25
At5g10270	CDKC;1	122	90	0.11
At1g74330	CKL2	53	31	0.20
At1g03740	CKL6	114	25	0.39
At5g44290	CKL5	200	46	0.57

Fig. 2. Transcript levels of core cell cycle regulators expressed during seed germination. Normalized signals (average signal at timepoint T/mean signal) of expressed genes (see *Materials and Methods*) are shown in a colored representation. Maximum (Max) and minimum (Min) detected signals and the coefficient of variation of expression are shown. A predominantly cream color in a row indicates genes that are relatively constantly expressed; orange to red represents down-regulated genes, and light to dark blue represents up-regulated genes. The box indicates "early" cell cycle regulators which peak at the end of phase I or in phase II, and contains six D-type and two A-type cyclins.

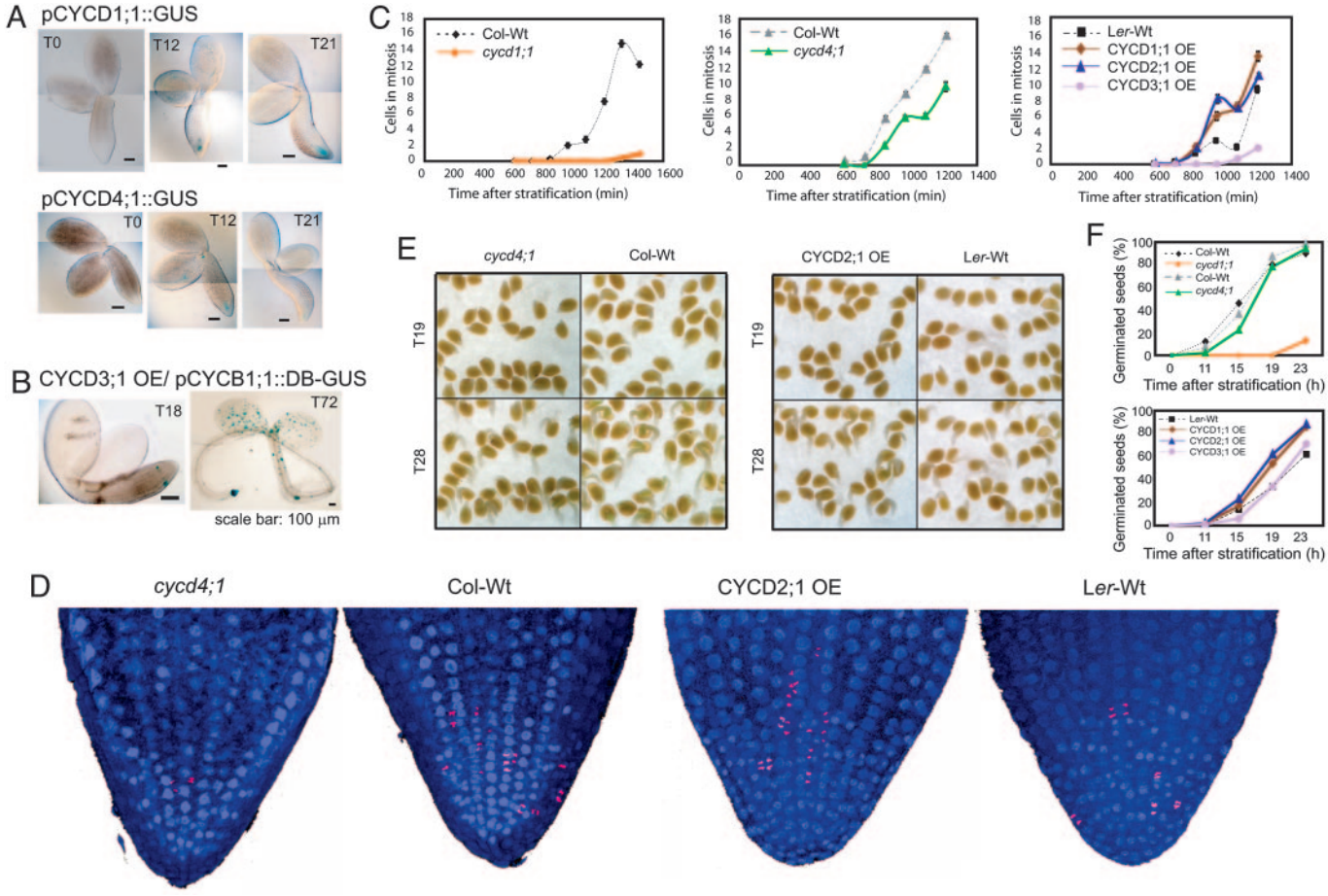

Fig. 3. Control of germination and cell cycle activation in the root apex by D-type cyclins. (*A*) Timing and localization of *CYCD1;1* and *CYCD4;1* expression in the RAM during germination using promoter-GUS fusions. Transcriptional activation of *CYCD1;1* (*Upper*) and *CYCD4;1* (*Lower*) in the center of the root tip 12 and 21 h after stratification, as revealed by the corresponding pCYCD::GUS reporters. *CYCD4;1* shows a transient activation 12 h after stratification, whereas *CYCD1;1* reaches its full activation at 21 h. Both results correlate with microarray analysis shown in Fig. 2. (*B*) *CYCD3;1* OE causes ectopic divisions in seedlings during phases III and IV (compare Fig. 1*A*), as shown by the mitotic marker pCYCB1::DB-GUS in seedlings homozygous for both constructs. (*C*) CYCD levels control the number of dividing cells during root meristem activation. *Cycd1;1* (*Left*) or *cycD4;1* (*Center*) loss-of-function homozygous mutants have delayed onset of cell division activity and fewer dividing RAM cells, resulting in a lower rate of cell division. Overexpression of early activated D-type cyclins such as *CYCD2;1* and *CYCD1;1* increases the number of cycling cells within the root apex (*Right*). Standard error of the mean is shown by error bars, but these are poorly visible because SE was <0.5 mitotic cells in all cases. Time axis is shown in minutes, and mitotic cells were determined up to 1,200 min (20 h; *Center* and *Right*) or 1,400 min (23 h, *Left*). Note that these time points precede the activation of ectopic divisions by *CYCD3;1* OE shown in *B Right*. (*D*) Distribution of mitotic figures in *cycd4;1* and control Col-WT roots segregated from the same parental population at 14 h, and *CYCD2;1* OE and L*er* WT control roots at 16 h, showing fewer mitotic cells in *cycd4;1* mutants and more in *CYCD2;1* OE. (*E*) Accelerated seed germination in CYCD2;1 OE (*Right*) and delayed germination in *cycd4;1* mutant (*Left*) compared to their respective WT controls observed at 19 and 28 h (T19, T28). (*F*) The initial rate of root protrusion in *CYCD1;1* and *CYCD2;1* OE seeds is increased compared to WT controls, and reduced in the normally later-activated *CYCD3;1* OE over a time course of 23 h.

in the two "early" D-type cyclins *cycd1;1* and *cycd4;1*, examined the rate and extent of cell cycle activation by scoring mitotic figures present in root tips during germination, and correlated this with the overall rate of germination as defined by radicle emergence. We found that, in root tips of *cycd4;1* mutant seedlings (Fig. 3 *C* and *D Left*) and in *cycd1;1* mutants, the onset of cell proliferation is significantly delayed and the overall numbers of dividing cells are reduced (Fig. 3*C*). Importantly, this delay in cell cycle activation is linked to delayed radicle emergence in these *cycd* mutants (Fig. 3 *E* and *F*), mirroring the effect of cell cycle inhibitors.

These mutant analyses suggest that *CYCD4;1* and *CYCD1;1* are rate-limiting for cell division in the root apex during germination, and that the delay in mitotic activation observed in these mutants leads to delayed radicle emergence. To further confirm the overall role of CYCD in controlling both mitotic activation and germination, we also examined mitotic activation and germination in constitutive OEs, available in our laboratory, of the early cyclins *CYCD1;1* and *CYCD2;1* and late cyclin *CYCD3;1*, predicting that, if germination is dose-responsive to CYCD expression level, we should observe more rapid germination. Scoring the number of cells in mitosis in the embryonic root tips, we found that the earliest cell divisions were observed at the same time after 12 h in *CYCD2;1* OE, *CYCD1;1* OE, and control roots (Fig. 3 *C* and *D*) but then the number of cycling cells rose much more rapidly in roots of both *CYCD2;1* and *CYCD1;1* OE seedlings than in WT (Fig. *3C*), especially in the central part of the root (Fig. 3*D*), leading to more rapid germination and radicle emergence (Fig. 3 *E* and *F*). Importantly, this is not a general effect of all CYCD, because the late activated *CYCD3;1* was unable to promote extra divisions in the root or faster root emergence during phase II (Figs. 3 *C* and *F*) and, indeed, delays germination significantly. *CYCD3;1* OE nevertheless is capable of promoting extensive ectopic divisions in other tissues such as the hypocotyl and elsewhere, extending cotyledon divisions into phase IV (Fig. 3*B*). Therefore, *CYCD3;1* OE leads to neither

faster RAM cell cycle activation nor more rapid germination (Fig. 3 *C* and *F*), but rather extends the period of division of cells in developmental contexts in which mitotic activity should have ceased, consistent with hyperplasia reported in older plants (28).

During seed formation, cells of the embryo arrest either only in the G_1 or in both G_1 and G_2 phase of the cell cycle, depending on the species (30, 31), with *Arabidopsis* showing an exclusively G_1 arrest (Fig. 1*B*). Faster cell cycle activation in CYCD OE could result from a higher proportion of cells in the dormant embryo arrested later in the cell cycle. However, WT, *CYCD2;1* OE, and *CYCD1;1* OE embryos all show arrest in G_1, as in WT seed (Fig. 6). Therefore, the higher number of cells in mitosis in *CYCD2;1* and *CYCD1;1* OE indicates that more RAM cells engage in the mitotic cell cycle when the levels of these CYCDs are elevated. In tobacco overexpressing *CYCD2;1*, a faster growth rate of plants was associated with a larger dividing cell population and shorter cell cycle duration (13).

Conclusion

In the dry *Arabidopsis* seed, cells of the embryo are arrested in the G_1 phase of the cell cycle. Germination is initiated by water uptake and the resumption of metabolic activity, and is regarded as complete once the radicle penetrates the seed coat. The mechanism responsible for radicle elongation during germination is controversial, and the generally accepted view is that initiation of DNA synthesis leading to either mitotic or endocycles only contributes to postgermination root growth (1, 3, 7). However, in some species, cell division has been detected before root protrusion, although any contribution of division to the germination process has not been determined (1, 7, 8).

Here we show that cell cycle activation within the root meristem precedes root protrusion, and using inhibitors that the activation of the cell cycle plays an important contributory role in driving the process of germination in *Arabidopsis*, in contrast to these previous views (7). Moreover, by genome-wide transcription profiling of gene expression during germination, we are able not only to define specific phases that link morphological changes and meristem activation with these expression profiles, but also identify candidate regulators of cell cycle activation that are expressed before radicle emergence. Indeed 10% of *Arabidopsis* genes show significant regulation before the activation of the root meristem.

Among these early activated genes are six CYCD genes, and these are shown to promote both cell cycle activation and the rate of germination when overexpressed, whereas *CYCD3;1*, a CYCD gene normally only activated postgermination is incompetent to promote root meristem activation. We have also identified loss-of-function mutants in two CYCD genes and show that both contribute to the rate of activation of cell division and the rate of germination. These subtle loss-of-function mutant phenotypes show that plant D-type cyclins have important additive effects in controlling the rate of cell-cycle activation, which then contributes directly to control of germination rate. We conclude that activation of cell division is a key determinant of germination in *Arabidopsis*, and that early-activated CYCD genes are rate-limiting controllers of germination rate that are therefore key regulators responding to the triggers for germination.

We thank Susan Howroyd for dedicated technical support and colleagues for helpful suggestions on the manuscript, Klaus Herbermann for important help with database design, and László Bögre and Catherine Perrot-Rechenmann as coordinators of the GVE (Growth, Vigour, Environment) and ACCY (Auxin and the Cell Cycle) Networks, respectively, for their efforts. This work was supported by the European Commission (EC) through the GVE Framework 5 RTD Network (QLK5-CT-2001-01871); the ACCY Framework 5 RTN Network (HPRN-CT-2002-00334) and a Marie Curie Incoming International Fellowship of the EC (509962) (to S.M.); and Biotechnology and Biological Sciences Research Council (BBSRC) Awards 8/G15864, C15792, and BBS/B/03815. N.H.M. was supported by a National Research Foundation of South Africa Fellowship, and C.C. was supported by a BBSRC Collaborative Award in Science and Engineering (CASE) award.

1. Bewley, J. D. & Black, M. (1994) *Seeds: Physiology of Development and Germination* (Plenum, New York).
2. Toorop, P. E., Barroco, R. M., Engler, G., Groot, S. P. & Hilhorst, H. W. (2005) *Planta* **221,** 637–647.
3. Bewley, J. D. (1997) *Plant Cell* **9,** 1055–1066.
4. Koornneef, M., Bentsink, L. & Hilhorst, H. (2002) *Curr. Opin. Plant Biol.* **5,** 33–36.
5. Gornik, K., Decastro, R. D., Liu, Y. Q., Bino, R. J. & Groot, S. P. C. (1997) *Seed Sci. Res.* **7,** 333–340.
6. Baiza, A. M., Vazquezramos, J. M. & Dejimenez, E. S. (1989) *J. Plant Physiol.* **135,** 416–421.
7. Barroco, R. M., Van Poucke, K., Bergervoet, J. H. W., De Veylder, L., Groot, S. P. C. Inze, D. & Engler, G. (2005) *Plant Physiol.* **137,** 127–140.
8. de Castro, R. D., van Lammeren, A. A., Groot, S. P., Bino, R. J. & Hilhorst, H. W. (2000) *Plant Physiol.* **122,** 327–336.
9. Dewitte, W. & Murray, J. A. H. (2003) *Annu. Rev. Plant Biol.* **54,** 235–264.
10. de Jager, S. M., Maughan, S., Dewitte, W., Scofield, S. & Murray, J. A. H. (2005) *Semin. Cell Dev. Biol.* **16,** 385–396.
11. Vandepoele, K., Raes, J., De Veylder, L., Rouze, P., Rombauts, S. & Inze, D. (2002) *Plant Cell* **14,** 903–916.
12. Wang, G. F., Kong, H. Z., Sun, Y. J., Zhang, X. H., Zhang, W., Altman, N., Depamphilis, C. W. & Ma, H. (2004) *Plant Physiol.* **135,** 1084–1099.
13. Cockcroft, C. E., den Boer, B. G., Healy, J. M. S. & Murray, J. A. H. (2000) *Nature* **405,** 575–579.
14. Riou-Khamlichi, C., Huntley, R., Jacqmard, A. & Murray, J. A. H. (1999) *Science* **283,** 1541–1544.
15. Rosso, M. G., Li, Y., Strizhov, N., Reiss, B., Dekker, K. & Weisshaar, B. (2003) *Plant Mol. Biol.* **53,** 247–259.
16. Alonso, J. M., Stepanova, A. N., Leisse, T. J., Kim, C. J., Chen, H. M., Shinn, P., Stevenson, D. K., Zimmerman, J., Barajas, P., Cheuk, R., *et al.* (2003) *Science* **301,** 653–657.
17. Colon-Carmona, A., You, R., Haimovitch-Gal, T. & Doerner, P. (1999) *Plant J.* **20,** 503–508.
18. Jefferson, R. A., Kavanagh, T. A. & Bevan, M. W. (1987) *EMBO J.* **6,** 3901–3907.
19. Bougourd, S., Marrison, J. & Haseloff, J. (2000) *Plant J.* **24,** 543–550.
20. Menges, M. & Murray, J. A. H. (2002) *Plant J.* **30,** 203–212.
21. Tavazoie, S., Hughes, J. D., Campbell, M. J., Cho, R. J. & Church, G. M. (1999) *Nat. Genet.* **22,** 281–285.
22. Eisen, M. B., Spellman, P. T., Brown, P. O. & Botstein, D. (1998) *Proc. Natl. Acad. Sci. USA* **95,** 14863–14868.
23. Gallardo, K., Job, C., Groot, S. P., Puype, M., Demol, H., Vandekerckhove, J. & Job, D. (2001) *Plant Physiol.* **126,** 835–848.
24. Planchais, S., Glab, N., Trehin, C., Perennes, C., Bureau, J. M., Meijer, L. & Bergounioux, C. (1997) *Plant J.* **12,** 191–202.
25. Sala, F., Parisi, B., Burroni, D., Amileni, A. R., Pedralinoy, G. & Spadari, S. (1980) *FEBS Lett.* **117,** 93–98.
26. Vazquez-Ramos, J. M. & Sanchez, M. D. (2003) *Seed Sci. Res.* **13,** 113–130.
27. Menges, M., De Jager, S. M., Gruissem, W. & Murray, J. A. H. (2005) *Plant J.* **41,** 546–566.
28. Dewitte, W., Riou-Khamlichi, C., Scofield, S., Healy, J. M. S., Jacqmard, A., Kilby, N. J. & Murray, J. A. H. (2003) *Plant Cell* **15,** 79–92.
29. Riou-Khamlichi, C., Menges, M., Healy, J. M. S. & Murray, J. A. H. (2000) *Mol. Cell. Biol.* **20,** 4513–4521.
30. Conger, B. V. & Carabia, J. V. (1978) *Environ. Exp. Bot.* **18,** 55–59.
31. Bino, R. J., Lanteri, S., Verhoeven, H. A. & Kraak, H. L. (1993) *Ann. Bot.* **72,** 181–187.